

## ORIGINAL ARTICLE

# Event attribution of Parnaíba River floods in Northeastern Brazil

Conrado Rudorff<sup>1</sup>  | Sarah Sparrow<sup>2</sup> | Marcia R. G. Guedes<sup>1</sup> | Simon. F. B. Tett<sup>3</sup> | João Paulo L. F. Brêda<sup>4</sup> | Christopher Cunningham<sup>1</sup>  | Flávia N. D. Ribeiro<sup>5</sup> | Rayana S. A. Palharini<sup>6</sup> | Fraser C. Lott<sup>7</sup>

<sup>1</sup> Centro Nacional de Monitoramento de Desastres Naturais, São José dos Campos, São Paulo, Brazil

<sup>2</sup> Oxford e-Research Centre, Engineering Science, University of Oxford, Oxford, UK

<sup>3</sup> School of Geosciences, University of Edinburgh, Edinburgh, UK

<sup>4</sup> Instituto de Pesquisas Hidráulicas, Universidade Federal do Rio Grande do Sul, Porto Alegre, Brazil

<sup>5</sup> Escola de Artes, Ciências e Humanidades, Universidade de São Paulo, São Paulo, Brazil

<sup>6</sup> Instituto Nacional de Pesquisas Espaciais, São José dos Campos, São Paulo, Brazil

<sup>7</sup> Met Office Hadley Centre, Exeter, Devon, United Kingdom

## Correspondence

Conrado Rudorff, Centro Nacional de Monitoramento de Desastres Naturais, São José dos Campos, São Paulo, Brazil.

Email: [conrado.rudorff@cemaden.gov.br](mailto:conrado.rudorff@cemaden.gov.br)

## Abstract

The climate modeling techniques of event attribution enable systematic assessments of the extent that anthropogenic climate change may be altering the probability or magnitude of extreme events. In the consecutive years of 2018, 2019, and 2020, rainfalls caused repeated flooding impacts in the lower Parnaíba River in Northeastern Brazil. We studied the effect that alterations in precipitation resulting from human influences on the climate had on the likelihood of flooding using two ensembles of the HadGEM3-GA6 atmospheric model: one driven by both natural and anthropogenic forcings; and the other driven only by natural atmospheric forcings, with anthropogenic changes removed from sea surface temperatures and sea ice patterns. We performed hydrological modeling to base our assessments on the peak annual streamflow. The change in the likelihood of flooding was expressed in terms of the ratio between probabilities of threshold exceedance estimated for each model ensemble. With uncertainty estimates at the 90% confidence level, the median (5% 95%) probability ratio at the threshold for flooding impacts in the historical period (1982–2013) was 1.12 (0.97 1.26), pointing to a marginal contribution of anthropogenic emissions by about 12%. For the 2018, 2019, and 2020 events, the median (5% 95%) probability ratios at the threshold for flooding impacts were higher at 1.25 (1.07 1.46), 1.27 (1.12 1.445), and 1.37 (1.19 1.59), respectively; indicating that precipitation change driven by anthropogenic emissions has contributed to the increase of likelihood of these events by about 30%. However, there are other intricate hydrometeorological and anthropogenic processes undergoing long-term changes that affect the flood hazard in the lower Parnaíba River. Trend and flood frequency analyses performed on observations showed a nonsignificant long-term reduction of annual peak flow, likely due to decreasing precipitation from natural climate variability and increasing evapotranspiration and flow regulation.

This is an open access article under the terms of the [Creative Commons Attribution](https://creativecommons.org/licenses/by/4.0/) License, which permits use, distribution and reproduction in any medium, provided the original work is properly cited.

© 2021 The Authors. *Climate Resilience and Sustainability* published by John Wiley & Sons Ltd on behalf of Royal Meteorological Society

## KEYWORDS

climate change, extreme weather events, flood risk, human influence, natural disasters

## 1 | INTRODUCTION

Climate change may be altering the frequency of hazards from extreme weather events such as heatwave, wildfire, drought, and flood at different rates across the globe (IPCC, 2014). Following an impactful extreme event, public awareness of the risk of natural disasters increases, intensifying questions about the role of climate change. Hence societies need scientific information to help them understand how they are being affected by climate change and clarify the drivers behind changes in the risk of hydrometeorological hazards. However, while the evidence of human influence on climate change is increasingly clear, tracing its effects on climate variability and extreme weather events needs more understanding (Stott, 2015; Easterling et al., 2016). The techniques for detection and attribution of extreme weather events have been developed for systematic assessments of the extent that anthropogenic climate change may be altering the probability or magnitude of impactful events (Stott et al., 2016; Ciavarella et al., 2018). An event attribution (EA) statement is based on a specific metric that characterizes the extreme nature of the event in question, being relevant for similar events in the future (Otto et al., 2016). Typical event definitions are of temperatures or rainfall averaged over a certain area and time to be above or below a threshold. The change in the likelihood of an extreme event resulting from human influences on the climate is usually expressed in terms of the ratio between probabilities of threshold exceedance in ensembles of atmospheric model simulations performed with and without the forcings of human influence on climate change (National Academies of Sciences, Engineering, and Medicine, 2016).

Initiatives such as [World Weather Attribution](#), an international effort to rapidly assess the attributable influence of climate change on extreme weather events, are using peer reviewed science and established methods to produce faster responses to the public, media, and decisionmakers (Black & Karoly, 2016; Karoly et al., 2016; Otto, 2016; Philip et al., 2020). Annual reports of the Bulletin of the American Meteorological Society (BAMS) on explaining extreme events of the previous year from a climate perspective are being published since 2012 (Zwiers et al., 2012), favoring the increase in the geographical coverage of EA studies. However, Central and South America, Africa, Western Asia, and Eastern Europe continue to feature a disproportional low number of published studies relative to the

other continental regions of the globe. Given the regional differences in dominant modes of internal variability and responses to external climate forcings, it is important to close gaps in global coverage for detection and attribution of climate extremes for the different types of events affecting livelihoods. Furthermore, disaster risk management often requires assessments on impact-related variables that are not included among the outputs of atmospheric models; therefore, requiring further modeling of land surface processes. For example, in dealing with droughts or floods, streamflow may need to be assessed using hydrological modeling (Philip et al., 2018; Ji et al., 2020). However, such numerical modeling cascade offers challenges associated to the effect of error propagation (Dams et al., 2015; Karlsson et al., 2016).

The Parnaíba River forms the border of the states of Maranhão and Piauí and is of great economic importance for agriculture and livestock farming in the Northeastern Brazil. Balancing the water supply-demand is the main challenge of water resources management for this semi-arid catchment. Research information is currently scarce on how climate change is expected to affect the streamflow of the Parnaíba River and challenge the existing water management strategies. The Parnaíba River experienced a major hydrological drought from 2012–2017 (Martins et al., 2018), while heavy rainfalls in 2018 caused flooding with impacts in states of Maranhão and Piauí. On April 18th, the Parnaíba River flow peaked at 3093 m<sup>3</sup>/s in Luzilândia, Piauí, corresponding to a 3-year return period flood. As the flood stage was exceeded, 4250 people were reported to become homeless or temporarily displaced across Luzilândia and three other towns in the lower Parnaíba River ([Secretaria Nacional de Proteção e Defesa, Civil](#)). The low return period and high number of people affected shows that a flood of this magnitude is not uncommon but causes relevant impacts due to population exposure and vulnerability (Rodrigues Neto and De Lima, 2019). Subsequent floods of slightly higher magnitude also occurred in 2019 and 2020. As common as these events may seem, it is vital to know whether they are becoming more frequent to guide development of adaptation and mitigation strategies that would decrease social and economic losses in such a vulnerable region.

There are intricate hydrometeorological and anthropogenic processes undergoing long-term changes that affect the flood hazard in the lower Parnaíba River. We investigate drivers of flood hazard change between 1982

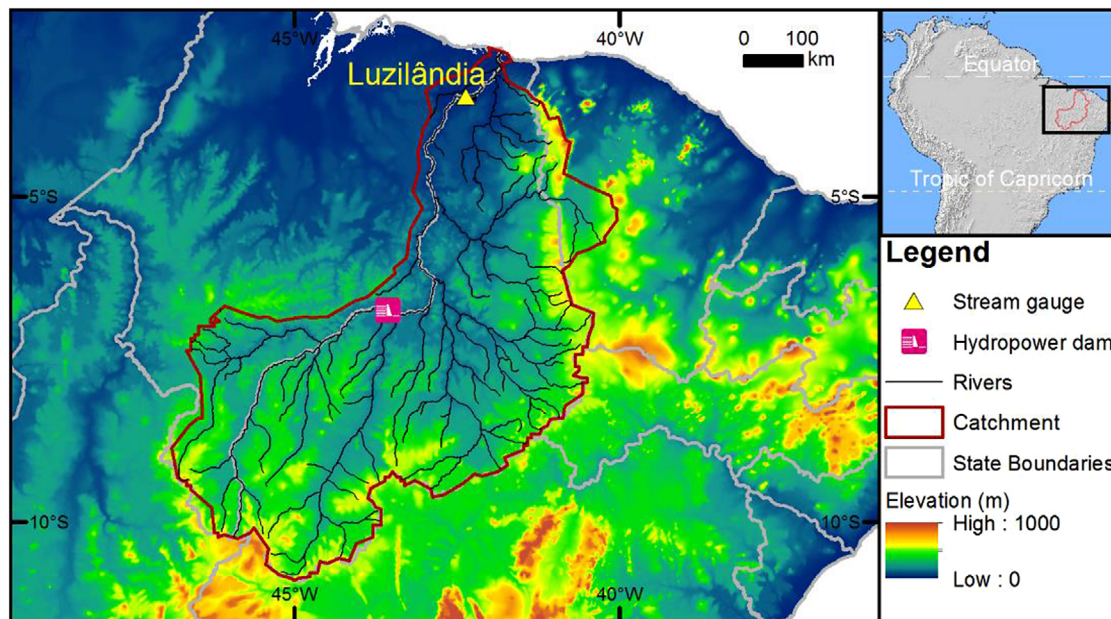


**FIGURE 1** Location of Luzilândia, Piauí in Northeastern Brazil that was impacted by flooding in 2018, 2019, and 2020. The delimitation of the Parnaíba River catchment, the main river network, the Boa Esperança hydroelectric dam, and the stream gauge (ID: 34879500) operated by the Brazilian National Water Agency (ANA) in Luzilândia are depicted

and 2020 based on observations of streamflow, precipitation, and river flow regulation by dams. Using the Hadley Centre's attribution modeling system (Ciavarella et al., 2018), we assessed the influence of anthropogenic climate change on flood hazard trend. We appraise daily precipitation as one of the drivers of change in flood hazard and performed hydrological modeling to base our assessments on the annual peak streamflow. Finally, we performed event attribution of the influence of anthropogenic climate change on the likelihood of flooding impacts in the lower Parnaíba River for the 2018, 2019, and 2020 events. The article is organized as follows: the main characteristics of the Parnaíba River catchment and rainfall mechanisms are introduced in Section 2; the approaches for observational trend detection and attribution modeling are presented in Section 3; the results are described and discussed in Section 4; and Section 5 concludes this study.

## 2 | STUDY SITE

Our study focuses on the lower reach of the Parnaíba River, near Luzilândia, Piauí (Figure 1), which drains a catchment area of about 325,000 km<sup>2</sup> in a tropical savanna climate with annual precipitation of about 980 mm. The rainfall is seasonal and almost totally from January to May with a late peak around March–April. The southward shift of the Intertropical Convergence Zone (ITCZ) during this time of the year is the main mechanism for the increase in rainfall

(Hastenrath, 2012). During this season upper tropospheric cyclonic vortices form in the tropical South Atlantic and frequently enter the continent near Salvador, Bahia (13°S 38°W). These vortices have a pronounced effect on the rainfall distribution over Northeastern Brazil, as their centers tend to suppress rainfall and their peripheries tend to favor heavy rainfall (Kousky and Gan, 1981; Mishra et al., 2007). At the subseasonal time scale, the Madden–Julian Oscillation (MJO; Madden and Julian, 1994; Zhang, 2005) modulates periods of enhancement and suppression of rainfall (de Souza and Ambrizzi, 2006; Alvarez et al., 2016).

The lower Parnaíba River features streamflow seasonality in response to the rainfall. Streamflow measured in Luzilândia remains low, at about 270 m<sup>3</sup> s<sup>-1</sup>, between July and October. High streamflow of about 1500 m<sup>3</sup> s<sup>-1</sup> occurs between March and April with median annual peaks of 2460 m<sup>3</sup> s<sup>-1</sup>. The observed streamflow peaks for the recent impact rendering 2018, 2019, and 2020 floods were 3093, 3377, and 3440 m<sup>3</sup> s<sup>-1</sup>, respectively (Figure 2).

Balancing the water supply-demand is the main challenge of water resources management for this semi-arid catchment. In the midreach of the Parnaíba River (43°30'W, 6°41'S), with an upstream catchment area of 87,500 km<sup>2</sup>, the Boa Esperança dam regulates flow for hydropower generation, water supply, irrigation, and flood control since 1970. About 36 other small reservoirs are also distributed in the basin, but despite river flow regulations both sides of the hydrological extremes commonly deliver significant socioeconomic impacts. A few



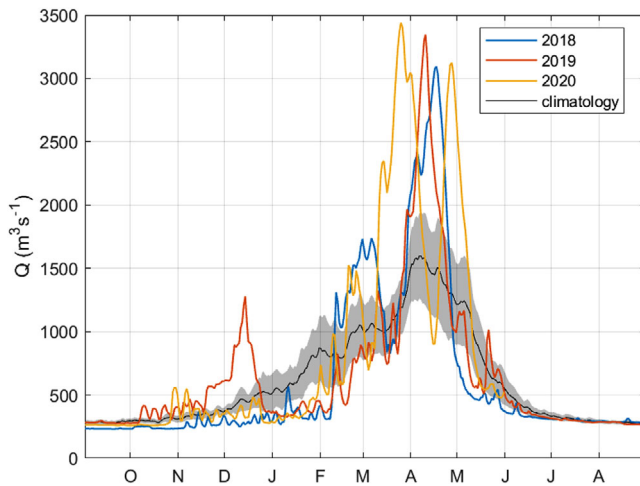


**FIGURE 2** Observed discharge ( $Q$ ) hydrographs that resulted in the 2018, 2019, and 2020 flooding in Luzilândia compared with the 1982–2020 climatology. Shaded areas are 95% confidence intervals estimated at each day of the year from the standard error of the median, multiplied by the calculated 95% values of the  $t$ -distribution, then adding and subtracting those values from the median. Stream gauge location is shown in Figure 1

studies reported on how climate change is expected to affect droughts of the Parnaíba River and challenge the existing water management strategies. Martins et al. (2018) performed an EA study of the 2012–2016 drought over the Northeastern Brazil and found no influence attributable to anthropogenic climate change. Based on a global water resources model of water use and availability, Palmer et al. (2008) suggested that the Parnaíba catchment is likely to experience a reduction in annual discharge of about 80% between the 1960s and 2050s with increasing water demand due to economic and population growth as the dominant driver rather than the effects of climate change. Historical increases and projections in water demand were confirmed in the impact assessment of five new dam projects that were approved to be built in the catchment (Collischonn et al., 2009). There are, however, still many open questions about how the risk of disasters from hydrological extremes may be changing due to changes in climate, catchment characteristics, water resources management, and population exposure. So far, to our knowledge, no comprehensive detection and attribution study of flood hazard change has been reported.

### 3 | METHODS

The following sections present the methods used to analyze observation-based flood trend and frequency and to perform the attribution modeling.

### 3.1 | Trend and flood frequency analyses based on observations

We apply the Mann–Kendall ( $\tau_A$ ) test to verify trends in time series. Statistically significant trends were defined as those having  $p < 0.05$ . The Sen's slope was used to estimate the magnitude of change. Furthermore, generalized extreme value (GEV) distributions of annual peak flows were fitted to estimate the probability of exceedance for peak discharge thresholds.

First, we analyzed flood trend and frequency based on annual peak streamflow observations available between 1982 and 2020 at the gauge operated by the National Water Agency (ANA) in Luzilândia (ID: 34879500). Then, we investigated total annual rainfall in the catchment and the influence of river flow regulation by dams as possible drivers of flood hazard change. The multi-source weighted-ensemble precipitation (MSWEP) (Beck et al., 2017) was used in our study as observational data for precipitation.

#### 3.1.1 | Influence of dams

The Boa Esperança Dam is currently the main structure regulating the flow of the lower Parnaíba River. The catchment area of the dam corresponds to 30% of the catchment area upstream to Luzilândia (Figure 1). We analyzed the dam outflow and naturalized flow (natural streamflow that would have occurred in the absence of water management in the catchment) to assess the dam influence on reduction of annual peak streamflow. These data were provided by the Operator of the National Electricity System ([Operador Nacional do Sistema Elétrico - ONS](#)). The natural flow estimates by ONS are based on water budget analysis that uses estimates of consumptive losses, including irrigation diversions, and reservoir evaporation, to quantify streamflow depletions. The estimated upstream depletions are then adjusted for the operation of reservoirs and added to the dam outflow (Wurbs, 2006). Reservoir evaporation is estimated based on the complementary relationship lake evaporation (CRLE) model (Morton, 1986) using observations from local meteorological stations. Hence, it includes the effect of local temperature increase due to global warming.

The probability ratio (PR), defined as the ratio of the probability of exceeding an event threshold in the dam outflow to the probability of exceeding the same threshold in the naturalized streamflow, was used to assess the influence of the Boa Esperança Dam. If the PR is greater than (less than) 1 then water management has increased (decreased) the likelihood of the event. If the PR is equal

to 1 then water management has not affected the chance of such an event occurring. To provide uncertainty estimates, we repeated the calculations of probabilities and PR by generating a 10,000-member bootstrap ensemble (Efron and Tibshirani, 1994). During each bootstrap ensemble member, the annual peak flow data were resampled with replacement (i.e., a value if chosen can be reselected) to get a set of new data with the same length as the original (Paciorek et al., 2018). The median instead of the mean value was used to avoid the influence of outliers, while the 5 and 95% percentiles provided uncertainty estimates at the 90% confidence level.

### 3.2 | Attribution modeling

Using the Hadley Centre's attribution modeling system (Ciavarella et al., 2018), we performed an attribution study of the influence of anthropogenic climate change on flood hazard trend. We appraised daily precipitation as the main driver of change in annual peak streamflow causing flood hazard and performed hydrological modeling to base our assessments on the annual peak streamflow. Finally, we performed specific event attribution assessments of the influence of anthropogenic climate change on the likelihood of flooding impacts in the lower Parnaíba River for the 2018, 2019, and 2020 events.

The Hadley Centre's attribution modeling system is comprised of two ensemble runs of the HadGEM3-GA6 atmospheric model with approximately 60 km resolution in mid-latitudes (Ciavarella et al., 2018): (i) the ALL ensemble, driven by both natural and anthropogenic forcings, with sea surface temperatures (SSTs) and sea ice coverage from HadISST (Rayner, 2003); and (ii) the NAT ensemble, driven only by natural atmospheric forcings and has anthropogenic changes removed from SST and sea ice patterns using the attribution methodology described in Pall et al. (2011) and Christidis et al. (2012). A pair of these ensembles with 15 members each, referred to as Historical and HistoricalNat, covers the period 1960–2013 and is used to validate the model and evaluate historical climatologies. For 2014–2016, seven members were branched from each simulation producing a pair of ensembles of size 105 and referred to as HistoricalShort and HistoricalNatShort. For 2016–onwards, a further five simulations were branched from each simulation, producing a pair of ensembles of size 525, referred to as HistoricalExt and HistoricalNatExt which have then been continued to date quasi-operationally on a seasonal basis. Further details of ensemble initialization, continuation, and attribution modeling framework are described in Ciavarella et al. (2018).

#### 3.2.1 | Atmospheric model evaluation and bias correction for precipitation

We compared daily climatologies from the HadGEM3-GA6 Historical ensemble median of 15 members against the MSWEP observed data for the period 1982–2013 to assess seasonal precipitation bias. The bias was quantified for each calendar month by the ratio between the model ensemble median and the observed time series. The correction was achieved by multiplying the Historical and HistoricalNat precipitation ensembles by the inverse of the bias ratio.

The performance of bias-corrected HadGEM3-GA6 precipitation over the catchment area was evaluated by applying the Index of Agreement (Willmott, 1981) to the model prediction of the Historical ensemble median of 15 members and the observational data of MSWEP for the period of 1982–2013. The Index of Agreement (IA) is defined as a standardized measure of the degree of model prediction error as:

$$IA = 1 - \frac{\sum_{i=1}^n (O_i - P_i)^2}{\sum_{i=1}^n (|P_i - \bar{O}| + \sum O_i - \bar{O})^2}, 0 < IA < 1, \quad (1)$$

where  $O_i$  is the observation value and  $P_i$  is the model prediction value and  $\bar{O}$  is the average observation value. The IA value of 1 indicates a perfect match, and 0 indicates no agreement.

#### 3.2.2 | Hydrological modeling

To relate the precipitation outputs from the HadGEM3-GA6 atmospheric model to streamflow as the flood impact-related measure, we ran simulations using the MGB (*Modelo hidrológico de Grandes Bacias*) hydrological model (Siqueira et al., 2018). The MGB is a semi-distributed, large-scale hydrological model designed for tropical catchments that simulates the terrestrial hydrological cycle, including soil water and energy budget, evapotranspiration, canopy interception, surface, subsurface and groundwater runoff, as well as flow routing along river channels. Evapotranspiration was simulated using the Penman–Monteith equation as a function of water availability simulated in soil and monthly climatologies (1961–1990) of temperature, pressure, radiation, and wind speed derived from the Climate Research Unit (CRU) Global Climate v.2 dataset at 10' resolution (New et al., 2002).

The performance of streamflow simulations was evaluated against gauge observations in Luzilândia (National Water, Agency) using the Nash–Sutcliffe efficiencies

(NSE), defined by Nash and Sutcliffe (1970) as:

$$\text{NSE} = 1 - \frac{\sum_{t=1}^N [Q_{\text{obs}}(t) - Q_{\text{sim}}(t)]^2}{\sum_{t=1}^N [Q_{\text{obs}}(t) - \overline{Q_{\text{obs}}}]^2}, \quad (2)$$

where  $Q_{\text{obs}}(t)$  is the observed discharge at time step  $t$ ,  $Q_{\text{sim}}(t)$  the simulated discharge,  $\overline{Q_{\text{obs}}}$  the mean observed discharge over the entire simulation period of length  $N$ . The NSE relates the mean square error generated by the hydrologic simulations to the variance of the observations, and can vary from  $-\infty$  to 1, where 1 would indicate a perfect match. Considering the strong and relatively constant seasonality of the hydrograph related to the climate, the interannual median value for every calendar day derived from observations was used as benchmark against which we compare the model performance (Schaeffli and Gupta, 2007). A skill score, scaled such that positive values indicate a model that is better than the benchmark model and negative values indicate a model that is worse than the benchmark model, was defined as:

$$\text{NSE}_{\text{skill score}} = \frac{\text{NSE}_{\text{model}} - \text{NSE}_{\text{benchmark}}}{1 - \text{NSE}_{\text{benchmark}}}. \quad (3)$$

Secondly, considering our focus on annual peak flows for flood frequency analysis, we used the metrics of percent bias (PBIAS) and root mean square error (RMSE) of annual peak flow. The percent bias measures the average tendency of the simulated values to be larger or smaller than their observed ones. The optimal value of PBIAS is 0.0, with low-magnitude values indicating accurate model simulation. Positive values indicate overestimation bias, whereas negative values indicate model underestimation bias.

$$\text{PBIAS} = 100 \times \left[ \frac{\sum_{y=1}^{n_y} (\text{peak}Q_{\text{sim}_y} - \text{peak}Q_{\text{obs}_y})}{\sum_{y=1}^{n_y} \text{peak}Q_{\text{obs}_y}} \right], \quad (4)$$

where  $\text{peak}Q_{\text{sim}}$  and  $\text{peak}Q_{\text{obs}}$  are the simulated and observed annual peak flow of year  $y$ , respectively, and  $n_y$  the number of simulated years.

### 3.2.3 | Trend and flood frequency analyses

Our evaluation of the influence of anthropogenic climate change on the flood trend and frequency was based on the annual peak streamflow of the Parnaíba River at Luzilândia simulated using the Historical and HistoricalNat precipitation bias-corrected ensembles of 15 members each,

covering the period of 1982–2013 (32 historical events). We applied the Mann–Kendall test and the Sen's slope estimator for the time series trend analyses. The assessment of human influence on the flood frequency integrated over the historical period was based on extreme value analysis and the probability ratio (PR). As the distributions of the 480 streamflow peaks were expected to be extreme in nature, GEV distributions were fitted and used to calculate the probability of exceeding the threshold value. The PR was defined as the ratio of the probability of exceeding the event threshold in the actual ensemble (Historical) to the probability of exceeding the same event threshold in the natural ensemble (HistoricalNat). If the PR is greater than (less than) 1, then human activity has increased (decreased) the likelihood of the event. If the PR is equal to 1, then human activity has not affected the chance of such an event occurring. To provide uncertainty estimates we repeated the calculations of probabilities and PR by generating a 10,000-member bootstrap ensemble (Efron and Tibshirani, 1994). During each bootstrap ensemble member, the annual peak flow data were resampled with replacement (i.e. a value if chosen can be re-selected) to get a set of new data with the same length as the original (Paciorek et al., 2018). The median value was used to avoid outliers, while the 5 and 95% percentiles provided uncertainty estimates at the 90% confidence level.

The streamflow of  $2700 \text{ m}^3 \cdot \text{s}^{-1}$  corresponds to the flood stage of the river in Luzilândia, established by the local civil defense authorities. Flood stage is typically defined as an established river gauge height for a given location at which a rise in water surface level begins to create a hazard to lives, property, or commerce. Given the relevance of the flood stage for flood risk management and

emergency response, a streamflow magnitude rounded to  $3000 \text{ m}^3 \cdot \text{s}^{-1}$  was selected as the threshold for our attribution study despite its low return period of 3 years. The probability of annual peak flow exceeding this threshold represents the probability of flooding that produces at least minor impacts.

### 3.2.4 | Event attribution

Finally, we assessed the influence of anthropogenic climate change on the likelihood of the 2018, 2019, and

**TABLE 1** Results of the statistical tests for trends (1982–2020) of: annual maximums of observed daily streamflow at the gauge in Luzilândia, total annual catchment precipitation, annual maximums of estimated daily naturalized flow and observed daily outflow of the Parnaíba River at the Boa Esperança Dam

Variable	Sen's slope	Lower CI	Upper CI	Mann-Kendall ( $\tau_A$ )	p value	Sig.
Annual peak streamflow observed in Luzilândia ( $\text{m}^3 \text{s}^{-1}$ )	−11.42	−49.24	26.05	−0.07	0.521	NS
Total annual catchment precipitation ( $\text{mm yr}^{-1}$ )	−0.65	−8.09	5.08	−0.01	0.923	NS
Naturalized flow at Boa Esperança Dam ( $\text{m}^3 \text{s}^{-1}$ )	−7.92	−20.98	3.47	−0.16	0.168	NS
Outflow from Boa Esperança Dam ( $\text{m}^3 \text{s}^{-1}$ )	−13.88	−27.35	−1.16	−0.26	0.020	*

\* $p < 0.05$ . NS, trend is not statistically significant at the 5% level. Increasing or decreasing trends are indicated by plus or minus signs of Sen's slope and  $\tau_A$  coefficient. Confidence intervals (CI) of Sen's slope are given at the 95% level. Locations of stations are indicated in Figure 1.

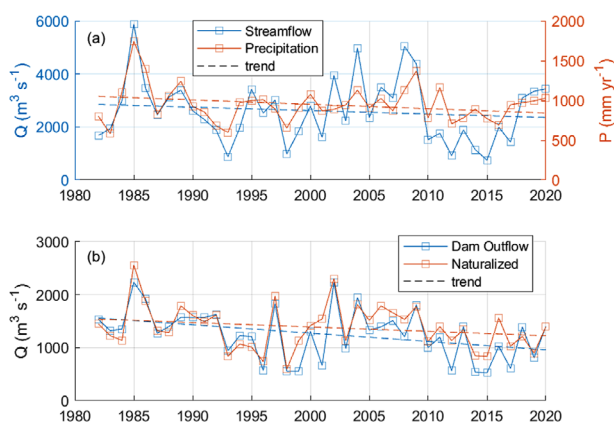


**FIGURE 3** (a) Total annual precipitation for the Parnaíba River catchment and annual peak streamflow in Luzilândia. (b) Annual peak outflow and naturalized flow of the Boa Esperança Dam

2020 flooding events following the risk-based approach of extreme event attribution (Otto, 2017). Here, we applied the same methodological procedure as described above but the change in likelihood of flooding was analyzed for each year individually. The event attribution was based on the HistoricalExt and HistoricalNatExt ensembles of 525 members each, with the correction for precipitation bias. The GEV distributions were fitted considering the 525 annual streamflow peaks simulated by the ensemble members for the specific year of analysis and used to calculate the probability of exceeding the threshold value. Hence, the prescribed SST and sea ice coverage were specific to the event of analysis.

## 4 | RESULTS AND DISCUSSION

### 4.1 | Trend and flood frequency analyses based on observations

The flood time series show a complex behavior varying at a range of time scales and floods are clustered in time (Fig-

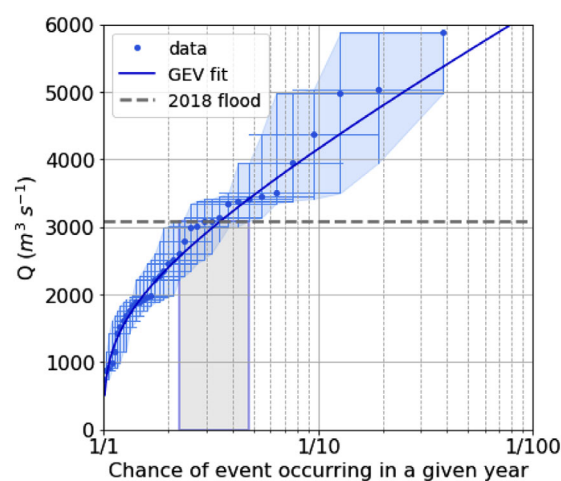


**FIGURE 4** Annual peak discharge versus return time from stream gauge observations in Luzilândia

ure 3a). Different moments of the time series behave differently, for example 2010–2017 and 2018–2020 were flood-poor and flood-rich periods, respectively, with reduced variability from year to year relative to the rest of the time series. In general, we found a nonsignificant decreasing flood hazard trend between 1982 and 2020 for the lower Parnaíba River based on observations of annual peak streamflow in Luzilândia (Sen's slope =  $-11.42 \text{ m}^3 \text{s}^{-1} \text{yr}^{-1}$ ; 95% CI =  $-49.24, 26.05$ ;  $\tau_A = -0.07$ ;  $p$ -value = 0.5214; Table 1).

GEV distributions of annual peak streamflow indicate return periods between 3 and 5 years for the 2018, 2019, and 2020 floods (Figure 4), which peaked at 3093, 3377, and 3440  $\text{m}^3 \text{s}^{-1}$ , respectively (Figure 2). The annual peak discharge was statistically correlated to annual rainfall with Pearson's  $r$  coefficients of 0.76 ( $p$  value  $< 0.001$ ). Precipitation is the main driver of flood hazard and showed a similar non-significant decreasing trend pattern (Sen's slope =  $-0.65 \text{ mm yr}^{-2}$ ; 95% CI =  $-8.09, 5.08$ ;  $\tau_A = -0.01$ ;  $p$ -value = 0.923) to peak annual discharge (Table 1, Figure 3a). Other important drivers of flood hazard change to consider for the lower Parnaíba are evapotranspiration and streamflow



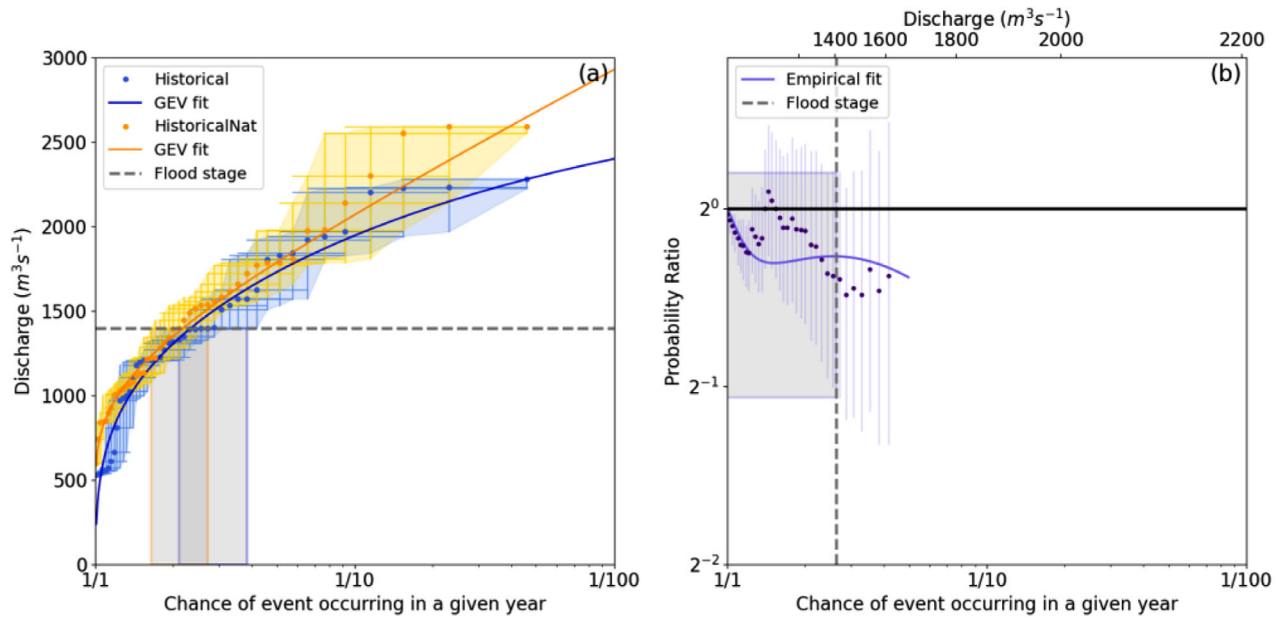


**FIGURE 5** (a) Annual peak discharge versus return time for the Boa Esperança dam outflow and the naturalized flow based on daily time series data between 1974 and 2020. (b) PR in terms of return time and magnitude. The solid black line indicates a PR of 1. PR calculations beyond the return time of one-in-five years are not shown as uncertainties were incomputable from the bootstrap ensemble. The dashed line corresponds to the peak dam outflow in 2018 in both plots

regulation. The atmospheric evaporative demand in Northeast of Brazil is increasing, mainly as a consequence of an increase in temperature (Da Silva, 2004). Increasing evaporation favors the decrease in streamflow peaks to an extent that has not yet been quantified for the Parnaíba River. To assess the influence of flow regulation on reduction of annual peak streamflow and possible trends, we analyzed the daily time series from 1982 to 2020 of the dam outflow and naturalized flow from the Boa Esperança Dam. A signal of long-term increase of dam influence is detectable by the significant decreasing trend in the annual maxima of dam outflow with a change of approximately 33% over the period from 1982 to 2020 (Sen's slope =  $-13.88 m^3 s^{-1} yr^{-1}$ ; 95% CI =  $-27.35, -1.16$ ;  $\tau_A = -0.26$ ;  $p$  value = 0.020), whereas no statistically significant trend was found for the annual maxima of naturalized flow (Sen's slope =  $-7.92 m^3 s^{-1} yr^{-1}$ ; 95% CI =  $-20.98, 3.47$ ;  $\tau_A = -0.16$ ;  $p$  value = 0.168; Table 1). The decrease in precipitation and increase in evaporation from reservoirs, catchment evapotranspiration, and water demand are likely the main factors causing the long-term increase of dam influence to soften these effects on stream flow variations. The GEV distribution of the annual peak dam outflow and naturalized flow were similar around the return time of one-in-three years (Figure 5a). The PR median (5% 95%) corresponding to the peak dam outflow in 2018 was 0.76 (0.48 1.15) (Figure 5b). The uncertainty bounds encompassed the value of 1 indicating that water management has not reduced the chance of such an event occurring.

The PR and uncertainty bounds were below 1 for events of return time lower than 1.5 years indicating reduction in the risk of such events due to dam attenuation of peak discharge. Beyond the return time of one-in-five years, PR uncertainties increased and were incomputable from the bootstrap ensemble. Our results corroborate with Passaia et al. (2020) who compared hydrological simulations that included forcing with historically observed dam outflow against simulations without the impact of dam flow regulation. Their modeling results indicated that the current water management practices reduced the 90th percentile of annual maximum discharge of the Parnaíba River in the reach immediately downstream of the Boa Esperança dam by 20%, but such dam influence diminished further downstream toward Luzilândia in the lower Parnaíba River.

The three factors that were discussed in this section as drivers of flood hazard trend (precipitation, evapotranspiration, and flow regulation) consistently support the finding of a nonsignificant flood hazard trend leaned towards reduction.

## 4.2 | Attribution modeling

### 4.2.1 | Atmospheric model evaluation and bias correction for precipitation

In our evaluation of HadGEM3-GA6 precipitation for the Parnaíba River catchment, we compared modeled



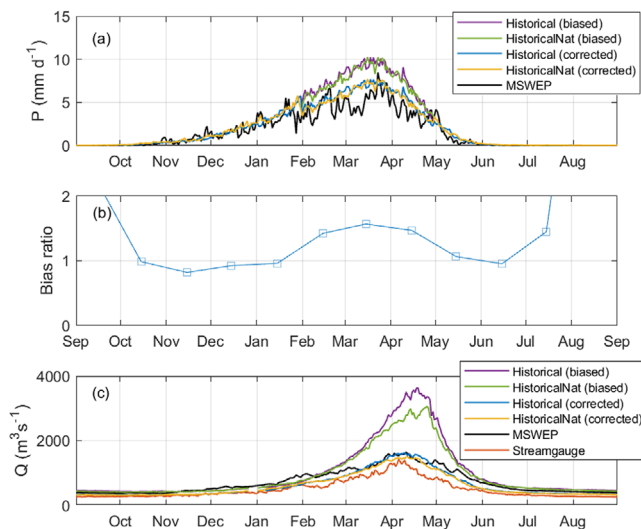


**FIGURE 6** (a) Daily median (1982–2013) precipitation over the basin from MSWEP and the medians of the 15 members from HadGEM3-GA6 Historical and HistoricalNat ensembles before and after bias correction. (b) Monthly variation of bias ratio between the median of HadGEM3-GA6 Historical ensemble and MSWEP. (c) Daily median (1982–2013) streamflow of the Parnaíba River in Luzilândia: stream gauge observations; hydrological simulations forced with precipitation from MSWEP, and median hydrological simulations forced with HadGEM3-GA6 Actual and Natural ensembles with and without bias

with observed climatologies over the hydrological year (September–August). The daily median (1982–2013) HadGEM3-GA6 historical ensemble was seasonally consistent with MSWEP observation (Figures 6a). A deviation in model precipitation during the wet season from February to April was repercussive to flood peak generation. The mean wet season (February–April) bias ratio between the HadGEM3-GA6 historical ensemble and MSWEP was calculated as 1.47. To correct for the model bias, the daily precipitation within the wet season was multiplied by the inverse of this bias ratio. The multiplicative correction using a constant value over the wet season adjusted the mean of the data, while preserving the trend and variability in relative terms. The Index of Agreement (IA) between the HadGEM3-GA6 Historical ensemble and MSWEP, as defined in the Methods section, increased from 0.59 to 0.78 after the bias correction (Figure 6a). The model bias was high from July to September (Figure 6b), but the differences in the low amounts of precipitation for this dry season period were small (Figure 6a). We consider the role of the MJO in modulating regional precipitation as connected with the HadGEM3-GA6 overestimation of precipitation during the wet season. The MJO is the main global mechanism modulating subseasonal variability in rainfall along the tropical belt. Following Wheeler and Hendon (2004), the MJO can be viewed as following

eight phases depending on the positioning of the rainy portion of the wave along the tropical belt. Convection is maximum in the western hemisphere and Africa during phases 8 and 1. Phases 2 and 3 correspond to enhanced convection over the Indian Ocean. Phases 4 and 5 peaks over the Maritime Continent, and phases 6 and 7 over the western Pacific. However, the canonical positioning of the suppressive portion of the MJO remains less ascertaining. Cunningham & Cavalcanti (2006) and Alvarez et al. (2016) reported evidence that, when the MJO convections is displacing from the Maritime Continent to the Western Pacific (phases 4 to 6), the northern South America (including the Parnaíba River watershed) is more likely to experience suppressed convection conditions. The pentad evolution of rainfall (MSWEP) shows two climatological dry spells. The first dry spell tends to occur from late-January to early-February, and the second in early-March (Figure 6a). Both happen during the wet season and by the time of the year when the MJO anomalies are strongest, December to March (Lafleur et al., 2015). To address whether those climatological dry spells in the Parnaíba River catchment are related to the suppressing phases 4 to 6, we performed an exploratory analysis on the historical series (1982–2013) of the daily real-time multivariate MJO index (RMM; Wheeler and Hendon, 2004). This analysis shows higher frequency of MJO's activity in phases 4–6 between mid-January and mid-March, concurrently to the climatological dry spell periods (Figure 7).

In general, climate models are not yet capable of producing accurate simulations of the MJO with the observable amplitude and systematic eastward propagation (Ahn et al., 2017). Walters et al. (2017) reported improvements in the MJO representation by HadGEM3-GA6 resulting from a calibration of the entrainment rate. However, the study did not evaluate the displacement of the MJO. Hence, we suggest that the model's overestimation of precipitation in Northeastern Brazil may, in part, be related to shortcomings in the representation of the MJO's suppressing effect during phases 4–6.

#### 4.2.2 | Hydrological modeling

The hydrological simulations forced by the HadGEM3-GA6 Historical precipitation without bias-correction overestimated streamflow at the gauge in Luzilândia, on average, by 89% for the February–April period, 52% higher than the precipitation overestimation (Figure 6). Such nonlinear rainfall-runoff response is common in arid river basins, mainly due to lower increase in evapotranspiration relative to precipitation during the rainfall events (Chiew, 2006). This effect highlights the additional challenge for event attribution studies on impact-related variables such

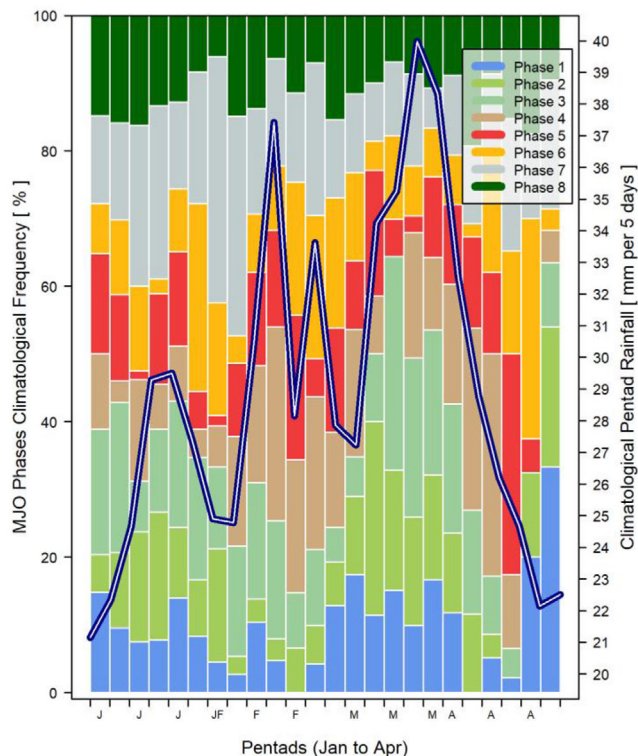


**FIGURE 7** Observed pentad time series (MSWEP; secondary y-axis) and frequency of the MJO phases (primary y-axis) over the Parnaíba basin. The blue-white line represents the long-term mean (1982–2013) of the accumulated precipitation for each pentad. There are 24 pentads between January and April (x-axis). The bars represent the frequency (counts per pentad) for each MJO phase. Phases commonly associated to rainfall in excess are colored with blue and green tones. Phases that tend to be associated with suppressed rainfall (4–6) are brown, red, and gold. Only MJO within the active category, that is, intensity greater than or equal to 1.5 (Lafleur et al., 2015) were considered

as streamflow, which require accurate estimates of meteorological variables when modeling further land surface processes.

After the bias correction of the HadGEM3-GA6 Historical ensemble, the streamflow overestimation was reduced to 1%. The daily median (1982–2013) streamflow hydrograph calculated from simulations forced by MSWEP and from the median of simulations results forced by HadGEM3-GA6 Historical ensemble were both comparable to stream gauge observations, peaking similarly around early-April (Figure 6c).

The daily flow series of the median HadGEM3-GA6 Historical ensemble (Figure 8) achieved the reasonable Nash–Sutcliffe efficiency (NSE) of 0.52. This value of NSE indicates that the model predicted substantially better than using the average of the observed data. The NSE of the hydrologic model is 30% higher than the NSE of the benchmark model (0.40). The performance improvement of the

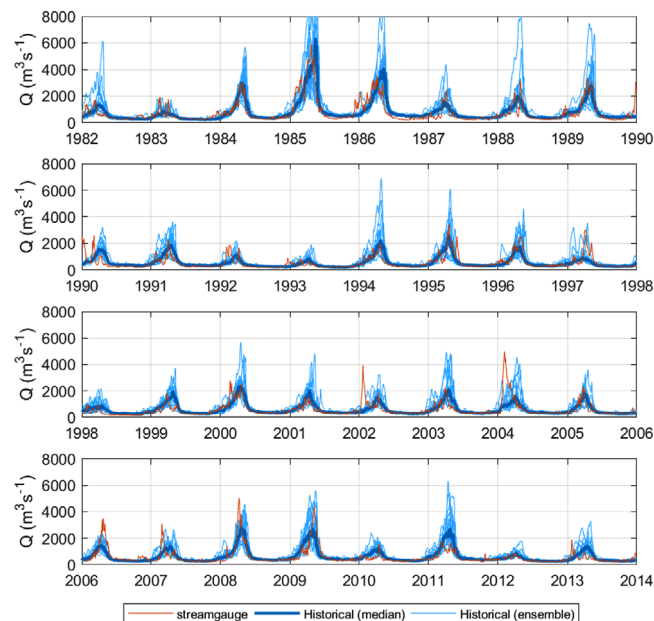


**FIGURE 8** Daily streamflow of the Parnaíba River in Luzilândia for 1982–2013: stream gauge observations; hydrological simulations forced with bias-corrected HadGEM3-GA6 Historical ensemble

hydrologic model over the benchmark model measured by the  $NSE_{skill\ score}$  was 0.20. This establishes that the hydrologic model has greater explanatory power than already contained in the seasonality of the climate. The percent bias (PBIAS) indicates underestimation of the HadGEM3-GA6 Historical ensemble median annual peak flow by 26% and the root mean square error (RMSE) is  $1212\text{ m}^3\text{ s}^{-1}$ . The underestimation of annual peak flow by the ensemble median was more pronounced in 1997, 2002, and 2004–2009. For 1997 and 2005–2009 the observed discharge peak was within the range of variability of the model ensemble, whereas in 2002 and 2004 the annual peak was observed early in the flood season and missed by all the ensemble members. The effects of long-term variations in potential evapotranspiration caused by the impacts of climate and land surface changes and of water resources management, such as dam operations and water extractions, were not represented in the hydrological model. Together with uncertainty in precipitation and other hydrologic parameters, these factors contribute to the differences between simulated and observed hydrographs. However, the reasonable performance achieved by the hydrologic model and the similar nonsignificant negative trends in observed time series of annual peak streamflow (Figure 9) and catchment rainfall (Figure 3a) suggest that the impacts of changes in evapotranspiration and dam operations on annual streamflow peaks were small in the lower Parnaíba River.

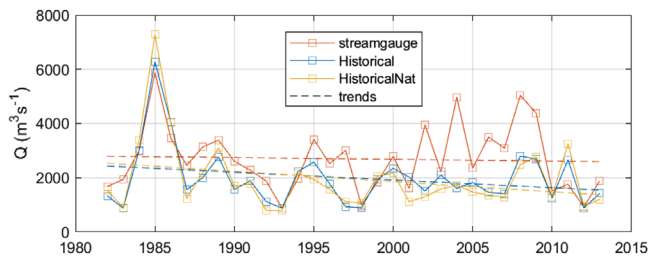


**FIGURE 9** Annual peak streamflow of the Parnaíba River in Luzilândia for 1982–2013: stream gauge observations; median from hydrological simulations forced with bias-corrected HadGEM3-GA6 Historical and HistoricalNat ensembles

#### 4.2.3 | Trend and flood frequency analyses

The annual peak flows in Luzilândia (1982–2013) simulated with the Historical and HistoricalNat ensembles of 15 members resulted in medians of similar interannual variation and negative nonsignificant trends (Historical ensemble median: Sen's slope =  $-13.07 \text{ m}^3 \text{ s}^{-1} \text{ yr}^{-1}$ ; 95% CI =  $-55.65, 23.23$ ;  $\tau_A = -0.10$ ;  $p$  value = 0.427; and HistoricalNat ensemble median:

Sen's slope =  $-15.80 \text{ m}^3 \text{ s}^{-1} \text{ yr}^{-1}$ ; 95% CI =  $-54.10, 18.23$ ;  $\tau_A = -0.11$ ;  $p$  value = 0.372; Table 2). These patterns were also similarly present in the stream gauge observations (Figure 9). The medians of annual peaks in the 1982–2013 period were 2087 and  $1835 \text{ m}^3 \text{ s}^{-1}$  for the Historical and HistoricalNat ensembles, respectively. The left-sided Wilcoxon rank sum test confirms the positive shift in the median due to anthropogenic forcings to be significant at the 5% level ( $p$  value of 0.044). The lower Sen's slopes of the HistoricalNat ensemble indicate that without anthropogenic climate change the decreasing trend of annual peak flow would be more pronounced while driven by natural climate variability. These results substantiate the model evaluation and point to changes in precipitation as the dominant driver of the trend of annual peak flow for the period. Martins et al. (2018) also concluded that natural climate variability is the main driver of a decreasing trend in precipitation in Northeastern Brazil.

GEV distributions of annual peak streamflow obtained from the Historical and HistoricalNat ensembles were also similar (Figure 10) with PR median (5%, 95%) of 1.12 (0.97, 1.26) at the flood impact threshold. This result points to a marginal contribution of anthropogenic emissions to an increase in likelihood of flooding by about 12%, with the lower PR uncertainty bound close to 1. The uncertainty in contribution of human influence increases towards more extreme floods with return time around one-in-ten-year.

Here the estimated probabilities for the ALL and NAT forcings scenarios are based on historical events of the 1982–2013 period. This allows similar interpretation to tra-

ditional flood frequency approach without preconditioning the SST to a specific year. The results are applicable to projects of hydrologic engineering planning and design, which requires stable information on the peak flows expected to be experienced at different likelihood levels. However, this historical context does not fully account for the present-day status of global warming, which may have important implications for flood risk management.

#### 4.2.4 | Event attribution

GEV distributions of the 2018, 2019, and 2020 annual maximum streamflows were fitted separately with data from each of the HistoricalExt and HistoricalNatExt ensembles of 525 members (Figure 11). The PR medians (5%, 95%) corresponding to the flood impact thresholds were 1.25 (1.07, 1.46), 1.27 (1.12, 1.445), and 1.37 (1.19, 1.59) for the 2018, 2019, and 2020 streamflow peaks, respectively (Figure 10b, d, and f). Hence, the event attribution analyses indicated that anthropogenic emissions have contributed to the increase in likelihood of these impact rendering floods in Luzilândia by about 30%. There is consistency in the results for these three years with different prescribed SST forcings that led to flood events with return periods of about one-in-four years. Risser et al. (2017) estimated year-to-year variability in calculations of the anthropogenic contribution to extreme weather based on ensembles of atmospheric model simulations. While providing results for the globe, they indicated the Northeastern Brazil to be among the few regions where the oceanic variability does not affect consistency of attribution statements for extreme rainfall events. A continued multi-year event attribution of peak flows of the Parnaíba River is desirable to quantify the possible positive trend in PR and further explore any dependence of anthropogenic influence on extreme floods to ocean variability.

Noteworthy towards a wider continental context is that human influence was attributed to cause a considerable fivefold increase in the risk of the April–May 2017 extreme rainfall (return period of 40 years) in the Uruguay River catchment in southern Brazil (Abreu et al., 2019). In contrast to the Parnaíba River, the Uruguay River presents a significant increasing trend of annual peak flow under a wet temperate climate of low rainfall seasonality.

## 5 | CONCLUSIONS

This study performed detection and attribution of climate extremes concerning floods in the lower Parnaíba River, Northeastern Brazil. Observations of annual catchment precipitation and peak discharge for the period 1982–2020

**TABLE 2** Results of the statistical tests for trends (1982–2013) of annual maximums of simulated daily streamflow ( $\text{m}^3 \text{s}^{-1}$ ) in the lower reach of the Parnaíba River near Luzilândia

Ensemble	member #	Sen's slope ( $\text{m}^3 \text{s}^{-1} \text{yr}^{-1}$ )	Lower CI	Upper CI	Mann-Kendall ( $\tau_A$ )	p value	Sig.
Historical	1	−77.77	−146.54	−12.57	−0.31	0.014	*
	2	20.79	−25.46	65.95	0.13	0.307	NS
	3	−24.27	−94.20	15.43	−0.15	0.236	NS
	4	11.22	−35.65	48.06	0.06	0.615	NS
	5	−56.22	−100.51	−3.92	−0.25	0.043	*
	6	−40.60	−113.89	17.07	−0.17	0.168	NS
	7	1.41	−42.62	41.76	0.00	0.987	NS
	8	−12.67	−62.07	23.97	−0.06	0.638	NS
	9	14.08	−29.37	53.47	0.10	0.427	NS
	10	4.17	−39.29	43.66	0.03	0.808	NS
	11	−15.98	−69.36	34.31	−0.08	0.549	NS
	12	−13.11	−70.99	33.22	−0.09	0.486	NS
	13	−16.18	−76.62	22.94	−0.10	0.408	NS
	14	−20.63	−71.48	25.84	−0.11	0.372	NS
	15	−20.37	−72.77	33.88	−0.14	0.277	NS
	Median	−13.07	−55.65	23.23	−0.10	0.427	NS
HistoricalNat	1	−13.18	−66.00	22.01	−0.09	0.486	NS
	2	−24.02	−87.52	12.31	−0.17	0.178	NS
	3	−23.48	−95.52	24.36	−0.12	0.339	NS
	4	−30.28	−85.64	5.30	−0.19	0.132	NS
	5	−9.95	−48.57	11.65	−0.09	0.486	NS
	6	−20.27	−68.53	18.63	−0.12	0.339	NS
	7	−3.32	−48.83	37.47	−0.02	0.858	NS
	8	2.23	−42.61	38.43	0.01	0.935	NS
	9	−30.52	−81.68	10.44	−0.19	0.132	NS
	10	−20.99	−67.46	12.53	−0.19	0.140	NS
	11	−24.45	−76.15	14.84	−0.13	0.323	NS
	12	−35.58	−101.09	8.21	−0.19	0.123	NS
	13	−5.83	−55.98	24.63	−0.03	0.833	NS
	14	−16.10	−55.22	15.92	−0.13	0.307	NS
	15	−16.10	−55.22	15.92	−0.13	0.307	NS
	Median	−15.80	−54.10	18.23	−0.11	0.372	NS

Abbreviation: NS, trend is not statistically significant at the 5% level.

\* $p < 0.05$ . Increasing or decreasing trends are indicated by plus or minus signs of Sen's slope and  $\tau_A$  coefficient. Confidence intervals (CI) of Sen's slope are given at the 95% level.

showed high correlation and non-significant decreasing trends. We analyzed outflow and naturalized flow of the upstream Boa Esperança Dam and found that flow regulation resulted in a low degree of flood peak attenuation, not having reduced the chance of floods with return time of 1.5–5 years significantly. Our analyses of historical observations indicate that the annual peak flow in the lower Parnaíba River has leaned towards reduction, driven by decreasing catchment precipitation, increasing flow reg-

ulation, and possibly also due to increasing atmospheric evaporative demand, but the overall long-term change is not detectable with statistical significance.

We used the HadGEM3-GA6 atmospheric model to investigate if the frequency of flooding is changing due to the influence of anthropogenic climate drivers on precipitation. We ran hydrological simulations to relate the precipitation outputs from the atmospheric model to streamflow as the flood impact-related measure. After



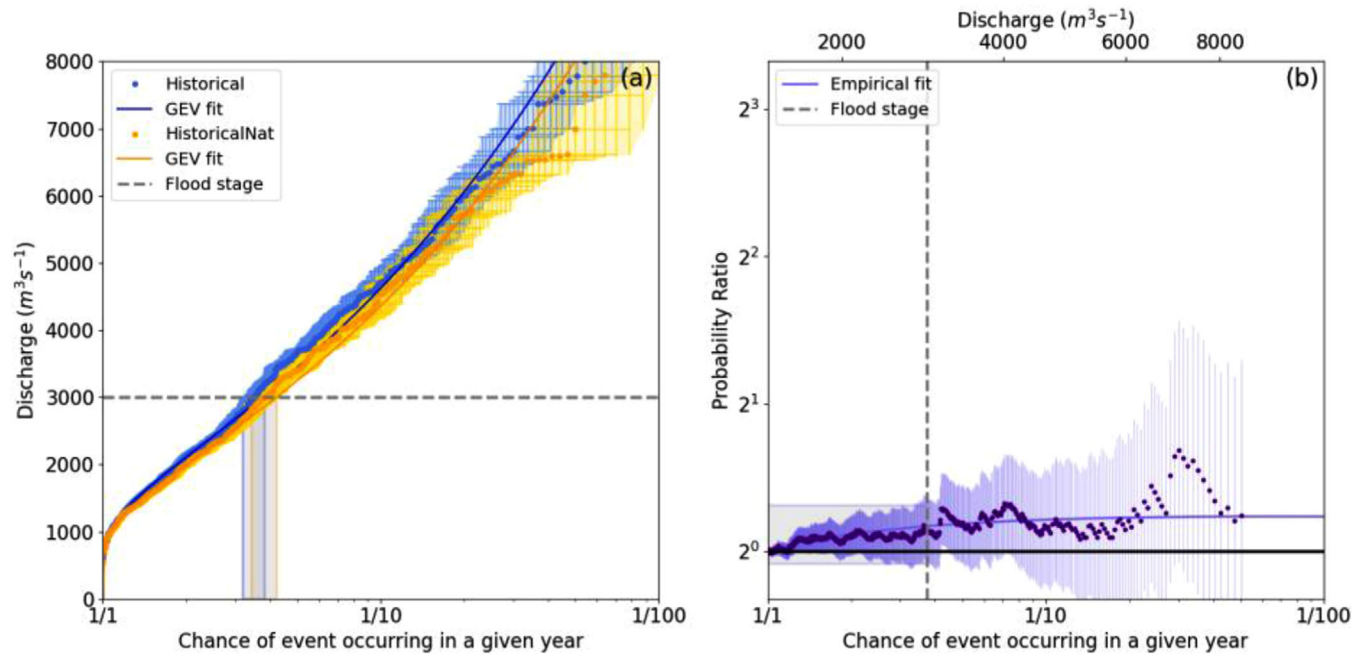


**FIGURE 10** Parnaíba River annual peak discharge in Luzilândia versus return time from hydrological simulations forced with bias-corrected HadGEM3-GA6 Historical and HistoricalNat ensembles. The corresponding probability ratio (b) in terms of return time and magnitude

precipitation bias correction, the streamflow simulations achieved a reasonable performance with greater explanatory power than already contained in the seasonality of the climate. The differences between simulated and observed hydrographs arouse from the uncertainty in precipitation and from the processes that were not modeled of water flow regulation by the dam and the long-term change in atmospheric evaporative demand. The historical trend, flood frequency, and event attribution analyses that were performed based on the climate and hydrological ensemble modeling led to the following main conclusions:

- The long-term (1982–2013) variation of annual peak flow of the lower Parnaíba River, simulated with the Historical and HistoricalNat ensembles of 15 members, were similar and showed a negative nonsignificant trend pattern like the stream gauge observations. Such pattern is related to the decreasing trend in precipitation over the region, which may be driven predominantly by natural climate variability.
- The probability ratio from flood frequency analyses of simulated events in the Historical and HistoricalNat ensembles (1982–2013), which integrate the impacts of changing SST and sea ice coverage over the period, indicated a non-significant increase in likelihood of flooding by 12% due to anthropogenic influences on climate.
- The event attribution analyses of three subsequent annual floods that impacted Luzilândia in 2018, 2019, and 2020 were performed individually, with flood proba-

bilities estimated from events generated by the extended ensembles of 525 members according to the specific SST and sea ice coverage prescribed for each year. The probability ratios indicated that anthropogenic climate change influence on precipitation increased the likelihood of these floods significantly by about 25, 27, and 37%, respectively. Taking account of uncertainty in the probability ratios these values are all consistent with one-another suggesting little variation in PR as function of the ocean state for the 2018–2020 period.

Authorities now have more scientific knowledge of the frequency and intensity of floods in this semi-arid catchment. The return periods of the 2018–2020 floods were low (3–5 years) relative to general flood risk protection standards but resulted in impacts in Luzilândia. This information by itself reveals the need of improvements in the local flood risk management strategies aiming to avoid future social and economic impacts. Thus, the flood events of 2018–2020 should be considered as case studies for developing disaster risk reduction actions to prevent the observed social and economic losses from happening into the future, particularly considering the high population vulnerability in the region. The lack of statistical significance of the trend in observed annual peak flow indicate that the current flood risk management decisions in the region may continue to be based on traditional flood frequency analysis of the peak streamflow climatology. However, considering our assessment of the positive

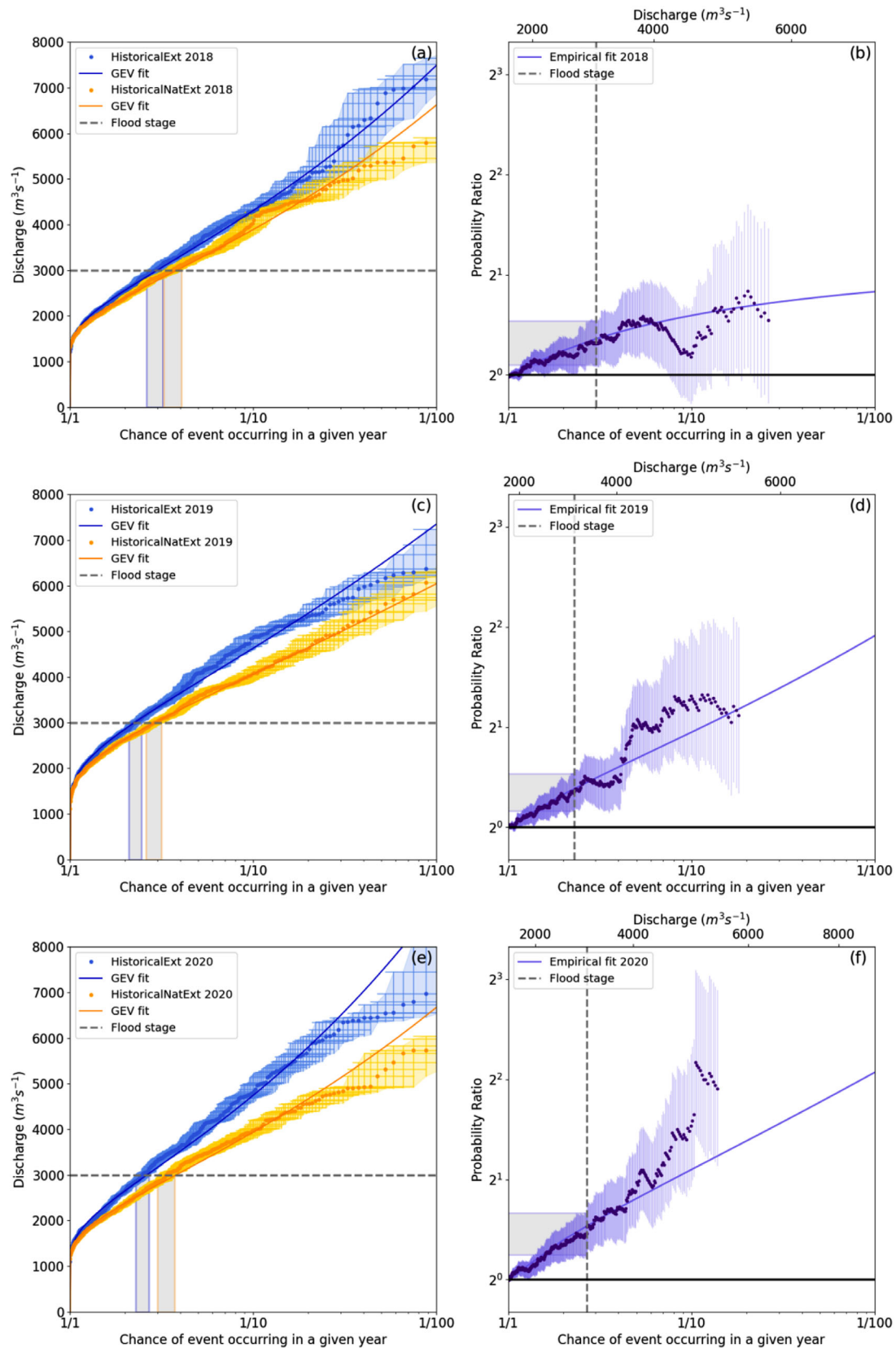


**FIGURE 11** (a) Parnaíba River 2018 peak discharge in Luzilândia versus return time of the HistoricalExt and HistoricalExtNat ensembles, and (b) the corresponding PR in terms of return time and magnitude. (c–d) Same as a–b but for 2019. (e–f) Same as a–b but for 2020. The dashed lines correspond to the threshold value of  $3000 \text{ m}^3 \text{ s}^{-1}$ , based on the peak streamflow in Luzilândia for 2018. The solid black line indicates a PR of 1. The line in each PR plot was fitted by calculating the PR based on the fits to the GEV distributions showing agreement with the median in the bootstrap, where well sampled


influence of anthropogenic climate change on the likelihood of flooding, we recommend continued event attribution assessment of future floods and investigation of flood hazard change based on climate projections. If a pattern of increase in variance of precipitation and peak discharge in a changing climate is confirmed to lead to flood hazard increase into the future, such result would support the need of climate change mitigation and adaptation policies. Arguably, adaptation and mitigation strategies have a particularly important role to play in reducing the risk of the more frequent but disruptive extremes events.

Finally, we point to two main actions of model improvement that will enhance attribution of greenhouse gas emission on flooding impacts: reduction of reliance in bias correction through continued improvements to the atmospheric model; and use of radiation, air temperature, humidity, and wind speed to account for the ongoing changes in atmospheric evaporative demand. The impact of increasing evapotranspiration on the magnitude of streamflow peaks is still to be investigated and quantified by future research. Furthermore, beyond the influence of anthropogenic climate change, the net change in flooding probability is also attributable to alterations in other factors related to catchment characteristics and water resources management. We recommend the incorporation of dam flow regulation processes into the runoff routing model to allow factoring the attribution of the impact of dams on flood events. Dam operations follow specific hydraulic rules but are constantly influenced by decisions based on various considerations affecting the regional power generation planning. The implementation of dam operation rules in the hydrological model is a task of increasing importance given the five new dam projects that have been approved to be built in the catchment.

## ACKNOWLEDGMENTS

This study resulted from a workshop on Operational Attribution at the University of Edinburgh sponsored by the Newton Fund through the Met Office's Climate Science for Service Partnership - Brazil (CSSP Brazil). MRGG & RSAP acknowledge support from CNPq, FNDR from FAPESP. SFBT and SS were funded by CSSP Brazil. The authors acknowledge the helpful review comments from Ruben Imhoff and a second anonymous referee.

## ORCID

Conrado Rudorff  <https://orcid.org/0000-0001-8453-1367>

Christopher Cunningham  <https://orcid.org/0000-0002-2235-8383>

## REFERENCES

- Ahn, M.-S., Kim, D., Sperber, K.R., Kank, I. - S., Maloney, E., Waliser, D. & Hendon, H. (2017) MJO simulation in CMIP5 climate models: MJO skill metrics and process oriented diagnostics. *Climate Dynamics*, 49, 4023–4045.
- Abreu, R.C., Cunningham, C., Rudorff, C.M., Rudorff, N., Abatan, A.A., Tett, S.F.B., Dong, B., Lott, F.C. & Sparrow, S.N. (2019) Contribution of anthropogenic climate change to April–May 2017 heavy precipitation over the Uruguay River Basin. *Bulletin of the American Meteorological Society*, 100, S37–S41. <https://journals.ametsoc.org/view/journals/bams/100/1/bams-d-18-0102.1.xml>.
- Alvarez, M.S., Vera, C.S., Kiladis, G.N. & Liebmann, B. (2016) Influence of the Madden Julian oscillation on precipitation and surface air temperature in South America. *Climate Dynamics*, 46, 245–262. <https://doi.org/10.1007/s00382-015-2581-6>.
- Beck, H.E., Van Dijk, A., Levizzani, V., Schellekens, J., Miralles, D.G., Martens, B. & Roo, A.D. (2017) MSWEP: 3-hourly 0.25° global gridded precipitation (1979–2015) by merging gauge, satellite, and reanalysis data. *Hydrology and Earth System Sciences*, 21, 589–615.
- Black, M.T. & Karoly, D.J. (2016) Southern Australia's warmest October on record: The role of ENSO and climate change. *Bulletin of the American Meteorological Society*, 97, S118–S121. <https://journals.ametsoc.org/bams/article/97/12/S118/215914/Southern-Australias-Warmest-October-on-Record-The>.
- Castro Cunningham, C.A. & De Albuquerque Cavalcanti, I.F. (2006) Intraseasonal modes of variability affecting the South Atlantic convergence zone. *International Journal of Climatology*, 26, 1165–1180. <http://doi.wiley.com/10.1002/joc.1309>.
- Chiew, F.H.S. (2006) Estimation of rainfall elasticity of streamflow in Australia. *Hydrological Sciences Journal*, 51, 613–625.
- Christidis, N., Scaife, A.A., Copsey, D., Jones, G.S., Stott, P.A., Arribas, A., Jones, G.S., Copsey, D., Knight, J.R. & Tennant, W.J. (2012) A new HadGEM3-a-based system for attribution of weather- and climate-related extreme events. *Journal of Climate*, 26, 2756–2783.
- Ciavarella, A., Christidis, N., Andrews, M., Groenendijk, M., Rostron, J., Elkington, M., Burke, C., Lott, F.C. & Stott, P.A. (2018) Upgrade of the HadGEM3-A based attribution system to high resolution and a new validation framework for probabilistic event attribution. *Weather and Climate Extremes*, 20, 9–32. <https://linkinghub.elsevier.com/retrieve/pii/S2212094717301305>.
- Collischonn, B., Pereira, P.R.G., Wanderley, R.M., Nóbrega, M.T. & Pante, A.R. (2009) *Declarações de Reserva de Disponibilidade Hídrica para os aproveitamentos hidrelétricos Ribeirão Gonçalves, Urucui, Cachoeira, Estreito e Castelhana, localizados no rio Paranaíba*. Brasília, DF.
- Dams, J., Nossent, J., Senbeta, T.B., Willems, P. & Batelaan, O. (2015) Multi-model approach to assess the impact of climate change on runoff. *Journal of Hydrology*, 529, 1601–1616. <https://doi.org/10.1016/j.jhydrol.2015.08.023>.
- Easterling, D.R., Kunkel, K.E., Wehner, M.F. & Sun, L. (2016) Detection and attribution of climate extremes in the observed record. *Weather and Climate Extremes*, 11, 17–27. <https://doi.org/10.1016/j.wace.2016.01.001>.
- Efron, B. & Tibshirani, R.J. (1994) *An introduction to the bootstrap*. London, UK: Chapman and Hall/CRC.
- Hastenrath, S. (2012) Exploring the climate problems of Brazil's Nordeste: A review. *Climatic Change*, 112, 243–251.

- IPCC (2014) Climate Change 2014: Impacts, Adaptation, and Vulnerability. Part A: Global and Sectoral Aspects. Contribution of Working Group II to the Fifth Assessment Report of the Intergovernmental Panel on Climate Change. In: Field, C.B., Barros, V.R., Dokken, D.J., Mach, K.J., Mastrandrea, M.D., Bilir, T.E., Chatterjee, M., Ebi, K.L., Estrada, Y.O., Genova, R.C., Girma, B., Kissel, E.S., Levy, A.N., MacCracken, S., Mastrandrea, P.R. & White, L.L. (Eds). Cambridge, UK and New York: Cambridge University Press.
- Ji, P., Yuan, X., Jiao, Y., Wang, C., Han, S. & Shi, C. (2020) Anthropogenic Contributions to the 2018 Extreme Flooding over the Upper Yellow River Basin in China. *Bulletin of the American Meteorological Society*, 101, S89–S94. <https://journals.ametsoc.org/bams/article/101/1/S89/346374/Anthropogenic-Contributions-to-the-2018-Extreme>.
- Karlsson, I.B., Sonnenborg, T.O., Refsgaard, J.C., Trolle, D., Børgesen, C.D., Olesen, J.E., Jeppesen, E. & Jensen, K.H. (2016) Combined effects of climate models, hydrological model structures and land use scenarios on hydrological impacts of climate change. *Journal of Hydrology*, 535, 301–317. <https://doi.org/10.1016/j.jhydrol.2016.01.069>.
- Karoly, D.J., Black, M.T., King, A.D. & Grose, M.R. (2016) The roles of climate change and El Niño in the record low rainfall in October 2015 in Tasmania, Australia. *Bulletin of the American Meteorological Society*, 97, S127–S130. <https://doi.org/10.1175/BAMS-D-16-0139.1>.
- Kousky, V.E. & Gan, M.A. (1981) Upper tropospheric cyclonic vortices in the tropical South Atlantic. *Tellus*, 33, 538–551.
- Lafleur, D.M., Barrett, B.S. & Henderson, G.R. (2015) Some climatological aspects of the Madden-Julian oscillation (MJO). *Journal of Climate*, 28, 6039–6053.
- Madden, R.A. & Julian, P.R. (1994) Observations of the 40–50-day tropical oscillation—A review. *Monthly Weather Review*, 122, 814–837. <http://journals.ametsoc.org/doi/abs/10.1175/1520-0493%281994%29122%3C0814%3A00TDTO%3E2.0.CO%3B2>.
- Martins, E., Coelho, C.A.S., Haarsma, R., Otto, F.E.L., King, A.D., Jan van Oldenborgh, G., Kew, S., Philip, S., Vasconcelos Júnior, F.C. & Cullen, H. (2018) A multimethod attribution analysis of the prolonged northeast Brazil hydrometeorological drought (2012–16). *Bulletin of the American Meteorological Society*, 99, S65–S69. <https://journals.ametsoc.org/doi/10.1175/BAMS-D-17-0102.1>.
- Mishra, S.K., Rao, V.B. & Franchito, S.H. (2007) Genesis of the northeast Brazil upper-tropospheric cyclonic vortex: A primitive equation barotropic instability study. *Journal of the Atmospheric Sciences*, 64, 1379–1392.
- Morton, F.I. (1986) Practical estimates of lake evaporation. *Journal of Climate and Applied Meteorology*, 25, 371–387. [http://journals.ametsoc.org/doi/10.1175/1520-0450\(1986\)025%3C0371:PEOLE%3E2.0.CO;2](http://journals.ametsoc.org/doi/10.1175/1520-0450(1986)025%3C0371:PEOLE%3E2.0.CO;2).
- Nash, J.E. & Sutcliffe, J.V. (1970) River flow forecasting through conceptual models part I - A discussion of principles. *Journal of Hydrology*, 10, 282–290.
- National Academies of Sciences Engineering and Medicine (2016) *Attribution of extreme weather events in the context of climate change*. Washington, DC: National Academies Press.
- National Water Agency. *Hidroweb*. Available at: <https://www.snirh.gov.br/hidroweb/serieshistoricas> (accessed March 23, 2021).
- New, M., Lister, D., Hulme, M. & Makin, I. (2002) A high-resolution data set of surface climate over global land areas. *Climate Research*, 21, 1–25.
- Operador Nacional do Sistema Elétrico. *Dados históricos observados nos reservatórios despachados pelo ONS*. Available at: <http://aplicam.ons.org.br/hidrologia/> (accessed March 23, 2021).
- Otto, F.E.L. (2016) The art of attribution. *Nature Publishing Group*, 6, 342–343. <https://doi.org/10.1038/nclimate2971>.
- Otto, F.E.L. (2017) Attribution of weather and climate events. *Annual Review of Environment and Resources*, 42, 627–646. <http://www.annualreviews.org/doi/10.1146/annurev-environ-102016-060847>.
- Otto, F.E.L., Van Oldenborgh, G.J., Eden, J., Stott, P.A., Karoly, D.J. & Allen, M.R. (2016) The attribution question. *Nature Climate Change*, 6, 813–816.
- Paciorek, C.J., Stone, D.A. & Wehner, M.F. (2018) Quantifying statistical uncertainty in the attribution of human influence on severe weather. *Weather and Climate Extremes*, 20, 69–80.
- Pall, P., Aina, T., Stone, D.A., Stott, P.A., Nozawa, T., Hilberts, A.G.J., Lohmann, D. & Allen, M.R. (2011) Anthropogenic greenhouse gas contribution to flood risk in England and Wales in autumn 2000. *Nature*, 470, 382–385. <http://www.nature.com/articles/nature09762>.
- Palmer, M.A., Reidy Liermann, C.A., Nilsson, C., Flörke, M., Alcamo, J., Lake, P.S. & Bond, N. (2008) Climate change and the world's river basins: Anticipating management options. *Frontiers in Ecology and the Environment*, 6, 81–89.
- Passaia, O.A., Siqueira, V.A., Brêda, J., Fleischmann, A.S. & de Paiva, R.C.D. (2020) Impact of large reservoirs on simulated discharges of Brazilian rivers. *RBRH*, 25, 1–9. [http://www.scielo.br/scielo.php?script=sci\\_arttext&pid=S2318-03312020000100212&tlng=en](http://www.scielo.br/scielo.php?script=sci_arttext&pid=S2318-03312020000100212&tlng=en).
- Philip, S., Kew, S., van Oldenborgh, G.J., Otto, F., Vautard, R., van der Wiel, K., King, A., Lott, F., Arrighi, J., Singh, R., & van Aalst, M. (2020) A protocol for probabilistic extreme event attribution analyses. *Advances in Statistical Climatology, Meteorology and Oceanography*, 6, 177–203.
- Philip, S., Sparrow, S., Kew, S.F., van der Wiel, K., Wanders, N., Singh, R., Hassan, A., Mohammed, K., Javid, H., Haustein, K., Otto, F. E. L., Hirpa, F., Rimi, R. H., Islam, A. K. M. S., Wallom, D. C. H., & van Oldenborgh, G. J. (2018) Attributing the 2017 Bangladesh floods from meteorological and hydrological perspectives. *Hydrology and Earth System Sciences Discussions*, 23, 1409–1429.
- Rayner, N.A. (2003) Global analyses of sea surface temperature, sea ice, and night marine air temperature since the late nineteenth century. *Journal of Geophysical Research*, 108, 4407. <http://doi.wiley.com/10.1029/2002JD002670>.
- Risser, M.D., Stone, D.A., Paciorek, C.J., Wehner, M.F. & Angélil, O. (2017) Quantifying the effect of interannual ocean variability on the attribution of extreme climate events to human influence. *Climate Dynamics*, 49, 3051–3073.
- Rodrigues Neto, E.X. & De Lima, A.J. (2019) Floods in Teresina-Piauí: A social-historical question. *Urbe*, 11, 1–14.
- Schaeffli, B. & Gupta, H.V. (2007) Do Nash values have value? *Hydrological Processes*, 21, 2075–2080. <http://doi.wiley.com/10.1002/hyp.6825>.
- Secretaria Nacional de Proteção e Defesa Civil. Relatório Gerencial - Danos informados. (Período: Abril, 2018; Desastre: Inundações; Estado: Piauí). <https://s2id.mi.gov.br/paginas/relatorios>.
- Da Silva, V. (2004) On climate variability in Northeast of Brazil. *Journal of Arid Environments*, 58, 575–596.
- Siqueira, V.A., Paiva, R.C.D., Fleischmann, A.S., Fan, F.M., Ruhoff, A.L., Pontes, P.R.M., Paris, A., Calmant, S., & Collischonn, W. (2018) Toward continental hydrologic-hydrodynamic modeling in



- South America. *Hydrology and Earth System Sciences*, 22, 4815–4842.
- de Souza, E.B. & Ambrizzi, T. (2006) Modulation of the intraseasonal rainfall over tropical Brazil by the Madden–Julian oscillation. *International Journal of Climatology*, 26, 1759–1776. <http://doi.wiley.com/10.1002/joc.1331>.
- Stott, P. (2015) Weather risks in a warming world. *Nature Climate Change*, 5, 516–517. <http://www.nature.com/articles/nclimate2640>.
- Stott, P.A., Christidis, N., Otto, F.E.L., Sun, Y., Vanderlinden, J.P., van Oldenborgh, G.J., Vautard, R., von Storch, H., Walton, P., Yiou, P., & Zwiers, F. W. (2016) Attribution of extreme weather and climate-related events. *Wiley Interdisciplinary Reviews: Climate Change*, 7, 23–41.
- Walters, D., Boutle, I., Brooks, M., Melvin, T., Stratton, R., Vosper, S., Wells, H., Williams, K., Wood, N., Allen, T., Bushell, A., Copsey, D., Earnshaw, P., Edwards, J., Gross, M., Hardiman, S., Harris, C., Heming, J., Klingaman, N., Levine, R., Manners, J., Martin, G., Milton, S., Mittermaier, M., Morcrette, C., Riddick, T., Roberts, M., Sanchez, C., Selwood, P., Stirling, A., Smith, C., Suri, D., Tennant, W., Luigi Vidale, P., Wilkinson, J., Willett, M., Woolnough, S. & Xavier, P. (2017) The Met Office Unified Model Global Atmosphere 6.0/6.1 and JULES Global Land 6.0/6.1 configurations. *Geoscientific Model Development*, 10, 1487–1520. <https://doi.org/10.5194/gmd-10-1487-2017>
- Wheeler, M.C. & Hendon, H.H. (2004) An all-season real-time multivariate MJO index: development of an index for monitoring and prediction. *Monthly Weather Review*, 132, 1917–1932. [http://journals.ametsoc.org/doi/10.1175/1520-0493\(2004\)132%3C1917:AARMMI%3E2.0.CO;2](http://journals.ametsoc.org/doi/10.1175/1520-0493(2004)132%3C1917:AARMMI%3E2.0.CO;2).
- Willmott, C.J. (1981) On the validation of models. *Physical Geography*, 2, 184–194.
- World Weather Attribution. <https://www.worldweatherattribution.org> (accessed March 18, 2021).
- Wurbs, R.A. (2006) Methods for developing naturalized monthly flows at gaged and ungaged Sites. *Journal of Hydrologic Engineering*, 11, 55–64.
- Zhang, C. (2005) Madden-Julian Oscillation. *Reviews of Geophysics*, 43, RG2003. [http://140.90.101.29/products/precip/CWlink/MJO/MJO\\_1page\\_factsheet.pdf](http://140.90.101.29/products/precip/CWlink/MJO/MJO_1page_factsheet.pdf).
- Zwiers, F., Hegerl, G.C., Min, S.-K. & Zhang, X. (2012) Explaining extreme events of 2011 from a climate perspective. *Bulletin of the American Meteorological Society*, 93, 1041–1067.

**How to cite this article:** Rudorff, C., Sparrow, S., Guedes, M.R.G., Tett, S.F.B., Brêda, J.P.L.F., Cunningham, C., Ribeiro, F.N.D., Palharini, R.S.A. & Lott, F.C. (2021) Event attribution of Parnaíba River floods in Northeastern Brazil. *Climate Resil Sustain*, 1–17. <https://doi.org/10.1002/cli2.16>.